DOI: 10.21513/2410-8758-2020-1-124-138 УДК 502/504:327.1

CURRENT CARBON DIOXIDE CONTENT IN THE NEAR-SURFACE LAYER OF THE EARTH'S ATMOSPHERE: LONG-TERM TRENDS AND INTRA-ANNUAL VARIABILITY

S.M. Semenov [1, 2, 3)*], *V.V. Kuzovkin* [1)]

[1)] Yu. A. Izrael Instiute of Global Climate and Ecology,
20b, Glebovskaya str., 107258, Moscow, Russian Federation;
*corresponding author: *SergeySemenov1@yandex.ru*

[2)] Institute of Geography, Russian Academy of Sciences,
29, Staromonetny per., 119017, Moscow, Russian Federation

[3)] Higher School of Economics – National Research University,
20, Myasnitskaya str., 101000, Moscow, Russian Federation

Abstract. The series of monthly mean concentrations of carbon dioxide (CO_2) in the near-surface layer of the atmosphere over the past 50 years have been analyzed. The series are presented on two publicly accessible Internet resources, namely, the websites of the World Greenhouse Gas Data Center (Global Atmosphere Watch, World Meteorological Organization) and of the Earth System Research Laboratory (National Oceanic and Atmospheric Administration, USA). The series from 80 stations are considered, of which 27 are from global (background) stations and the rest are from regional stations. Long-term changes are characterized by the series of twelve-month running averages, while intra-annual (inter-monthly) variability is described by the difference of the initial series and the series characterizing long-term changes. Consideration of systematic differences showed that the highest levels of CO_2 are characteristic of the regions with developed economies located in North America, Western and Central Europe, and Southeast Asia. Long-term changes (trends) at all stations are practically identical to those at the global (background) stations. Intra-annual variability is regular (seasonal). Seasonal deviations from the line of long-term trends at different points of geographical space demonstrate high correlative similarity after respective seasonal time shifts have been applied. Such similarity is manifested even at the long distance between the stations. The root-mean-square values of the series of intra-annual deviations are maximum in the regions with developed economies located in North America and Western and Central Europe. They are smaller in the high latitudes of the Northern Hemisphere, while in the Southern Hemisphere they are noticeably smaller and decrease with latitude.

Keywords. Carbon dioxide, near-surface concentrations, monitoring data, long-term changes, intra-annual variability, global analysis.

Introduction

Anthropogenic emissions of greenhouse gases significantly enrich the atmosphere with these substances. This enhances the greenhouse effect**,** thus favoring the global warming and concomitant changes in other climate parameters. As many of its consequences are evaluated negatively, the concerned world community applies joint efforts to studying these consequences (IPCC, 2018) and to limiting global climate change (UNFCCC, 1992; Kyoto Protocol, 1997; Paris Agreement, 2015).

To substantiate relevant measures, it is necessary to have reliable information on the global anthropogenic emissions of greenhouse gases and trends in their atmospheric content variation. Information on global anthropogenic emissions is collected in countries and submitted annually to the Secretariat of the UN Framework Convention on Climate Change (UNFCCC). Major international research projects are underway to evaluate greenhouse gas emissions from the Earth's surface to the atmosphere. For example, the Global Carbon Project aims at the assessment of the global budgets of carbon dioxide, methane, and nitrous oxide (see, for example, (Le Quéré et al., 2018)). Among the constituents of anthropogenic emissions, these greenhouse gases have the greatest radiative forcing.

Information on the levels of greenhouse gases in the atmosphere is collected at the monitoring stations where respective measurement programs are implemented. It is annually summarized in the publications of the World Meteorological Organization (see, for example, (The State of Greenhouse Gases ..., 2018)). At the national level, the United States (stations of the National Oceanic and Atmospheric Administration, NOAA) and Australia (the stations of the Commonwealth Scientific and Industrial Research Organization, CSIRO) have the most numerous networks of such stations. At the international level, a significant part of national monitoring stations is integrated into the Global Atmosphere Watch (GAW) network under the auspices of the World Meteorological Organization (WMO). These stations, located on the continents and islands in the ocean, characterize the content of greenhouse gases in the near-surface layer of the atmosphere.

Station observational data are stored in the GAW/WMO World Data Center for Greenhouse Gases (WDCGG) and national databases, including the database of the Earth System Research Laboratory (ESRL), USA. The WDCGG is operated by the Japan Meteorological Agency (JMA). The https://gaw.kishou.go.jp/ resource contains data on the levels of CO_2, CH_4, N_2O, and some other greenhouse gases in the near-surface atmosphere. The ESRL operates within the US National Oceanic and Atmospheric Administration. These data are obtained during *in situ* measurements or subsequent laboratory analysis of air samples taken with special containers.

The purpose of this article is to analyze the station series of monthly mean data on CO_2 content in the near-surface layer of the atmosphere available at the public domain of WDCGG and ESRL websites and to assess the global geographical distribution of:

– long-term trends in CO_2 monthly mean concentrations in the near-surface layer of the atmosphere;

– parameters of variability remaining after long-term trends have been eliminated from the series of monthly data.

Data and Methods

Systematic measurements of CO_2 content in the near-surface layer of the atmosphere began in the second half of the 20th century. This event is associated with the name of C.D. Keeling (Keeling et al., 2005), who has performed such measurements at Mauna Loa Station (Hawaii, USA) since 1958. Historical background can be found in (Semenov, 2018a).

At present, the GAW/WMO World Greenhouse Gas Data Center provides monthly mean CO_2 values of the surface atmosphere from 80 monitoring stations (more precisely, 76, because 4 stations are duplicated, that is they appear simultaneously in the CSIRO and NOAA databases; the series demonstrate up to 2% differences in some cases). Figure 1 shows the stations. Some of them (26 stations) have the status of global stations. We will assume that they represent the global background content of substances in the near-surface layer of the atmosphere. The others have the status of regional stations, i.e., represent a regional background. A list of global stations used in this article to characterize the global background content of CO_2 is given in Table 1.

Table 1. Global monitoring stations (https://www.esrl.noaa.gov/gmd/dv/data/)

Name	Latitude, degree	Longitude, degree	Elevation a.s.l., m	Country of affiliation or location
Cape Grim	-40.68	144.69	94	Australia
Assekrem	23.27	5.63	2710	Algeria
Barrow	71.32	-156.61	11	USA
Halley	-75.57	-25.50	30	USA
Tenerife	28.31	-16.50	2373	Spain
Mace Head	53.33	-9.90	5	Ireland
Mauna Loa	19.54	-155.58	3397	USA
Samoa (Cape Matatula)	-14.25	-170.56	77	USA
South Pole	-90.00	-24.80	2841	USA
Mt. Waliguan	36.29	100.90	3810	China
Zeppelin Mountain	78.91	11.89	475	Norway
Monte Cimone	44.17	10.68	2165	Italy
Cape Point	-34.35	18.49	230	South Africa
Minamitorishima	24.29	153.98	7	Japan
Mt. Kenya	-0.06	37.30	3678	Kenya
Bukit Kototabang	-0.20	100.32	864	Indonesia

Ushuaia	-54.85	-68.31	18	Argentina
Trinidad Head	41.05	-124.15	107	USA
Arembepe	-12.77	-38.17	0	Brazil
Alert	82.50	-62.34	210	Canada
Cape Rama	15.08	73.83	60	India
Casey	-66.28	110.52	47	Antarctic
Estevan Point	49.38	-126.53	7	Canada
Mawson	-67.62	62.87	32	Antarctic
Macquarie Island	-54.48	158.97	6	Australia
Shetland Islands	60.09	-1.26	30	Scotland

Let $\{A\ (n)\}$ denotes a station series of monthly mean concentrations. For this station, $n = 1$ corresponds to the month when the average monthly concentration was estimated for the first time, and $n = N$ corresponds to the serial number of the last month for which the average monthly concentration is available. The numbering of the months is continuous. Thus, for some months, the values of average monthly concentration may be absent. The data analysis method described below is a modification of the methodology proposed in (Semenov, 2018b) and applied to the analysis of CO_2, CH_4, and N_2O series in (Semenov, Ran'kova, 2018).

Next, let us denote by $\{B\ (n)\}$ a series of twelve-month running averages corresponding to $\{A\ (n)\}$ (for the illustration see Fig. 2):

$$B(n) = [0.5\ A(n - 6) + A(n - 5) +...+ A(n + 5) + 0.5\ A(n + 6)] / 12.$$

The $B\ (n)$ values are calculated only for those months for which the $A\ (n)$ values for the n-th month, the previous 6 months, and the next 6 months are available. When calculating the running average, differences in the duration of the calendar months are not taken into account.

It is the $\{B\ (n)\}$ series that is used to represent the long-term trend in monthly mean concentration (the trend is non-linear). However, the absolute values of concentrations at different monitoring stations may have systematic differences due to the characteristics of those parts of the geographical space where the stations are located. Therefore, to compare changes at different stations, these differences should be eliminated. In this work, this is achieved by 'adjusting' twelve-month moving averages at all stations under consideration to the values for the Alert station, the northernmost station in the Northern Hemisphere (82.5°N; 62.34°W). Namely, for a given station, the months are determined for which there are $B\ (n)$ values both for this station and for the Alert station. For this set of months, the average monthly mean concentrations are calculated for the given station ($\overline{B}$) and for the station Alert ($\overline{B}_{Alert}$). Further, the difference $\Delta\overline{B} = (\overline{B}_{Alert} - \overline{B})$ is added to all elements of $\{B(n)\}$ series for the considered station. The resulting adjusted series is denoted as $\{B^*(n)\}$. The choice of the Alert station for this operation is quite arbitrary. Its advantage is a fairly complete series of data and undoubtedly global background character (as it is a high-latitude Arctic station).

Figure 1. Stations that monitor CO_2 content in the near-surface layer of the atmosphere and whose data are used in this article. Some names are not shown (for example, in Western Europe) due to the lack of space in the panel

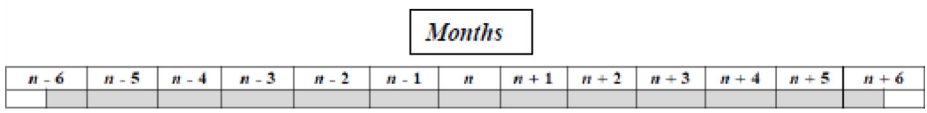

Figure 2. The gray color indicates the time interval used in calculating the running twelve-month average corresponding to the *n*-th month; the values for the first and the last months are included with the coefficient of 0.5

To describe the short-term variability of monthly mean concentration, the series $\{C(n)\}$, $C(n) = A(n) - B(n)$ is employed. Of course, its values are determined only for those n for which there are corresponding values of $A(n)$ and $B(n)$. The series $\{C(n)\}$ represents the variability of monthly average concentrations remaining after we have eliminated the long-term trend described by the series $\{B(n)\}$.

In this work, we will compute root-mean-square values for series $\{C(n)\}$ for the stations under consideration, as well as the correlations of these series for different pairs of stations. However, on calculating the correlations, time shifts of series will be applied: for $k \geq 0$, the series $\{C(n+k)\}$ is obtained by shifting the original series $\{C(n)\}$ by k months towards the earlier dates, and the series $\{C(n-k)\}$ for k months towards the later dates, respectively. For an ordered pair of series, the optimal shift is the shift of the second series by a number of months from (-5) to 6 which provides the maximum correlation of the series.

Results and discussion

Long-term trends and absolute levels of CO_2 content

Fig. 3 shows the long-term trends of monthly mean CO_2 concentrations represented by series $\{B^*(n)\}$ for 5 regional stations: Deuselbach (Germany), Diabla Gora (Poland), Kollumerwaard (Netherlands), Issyk-Kul (Kyrgyzstan), and

Constanta (Romania), as well as the average trend for the series of global background stations (the red line). These five stations have the maximum values of absolute deviations from the average global background trend that exceed 5 ppm. We qualify them as 'abnormal' and exclude from the further consideration.

In Figs. 4a-d, the red line shows the average trend (GB) for the series from global background stations. Each panel also has respective individual trend lines, graphs of the $\{B^*(n)\}$ series, characterizing long-term trends for all stations (G), North American stations (NA), European stations (EU), and Asian stations (AS). They are shown in blue. These individual lines are made thicker, and the red line is made intermittent, otherwise the graphs would be practically indistinguishable, since they deviate from the red line by only < 1-2 ppm. Thus, all the depicted trend lines characterizing the long-term trends in Fig. 4 almost coincide.

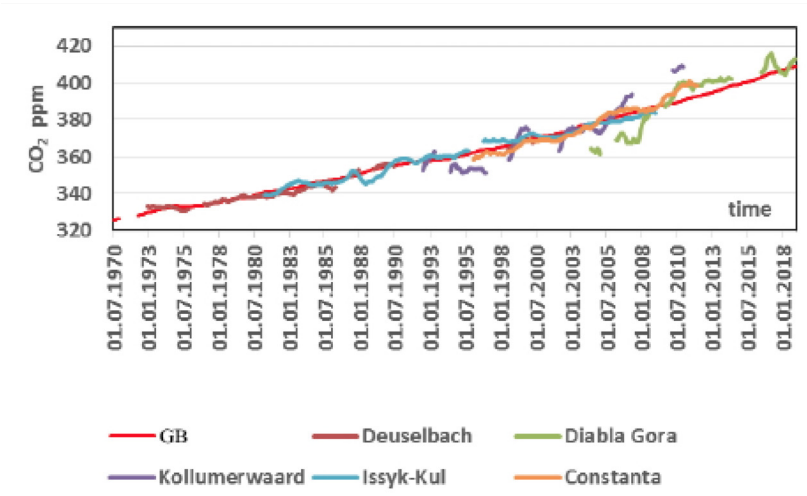

Figure 3. Average long-term trend (GB) of CO_2 content (ppm) in the near-surface layer of the atmosphere at the global background monitoring stations and individual long-term trends at the stations Deuselbach, Diabla Gora, Kollumerwaard, Issyk-Kul and Constanta

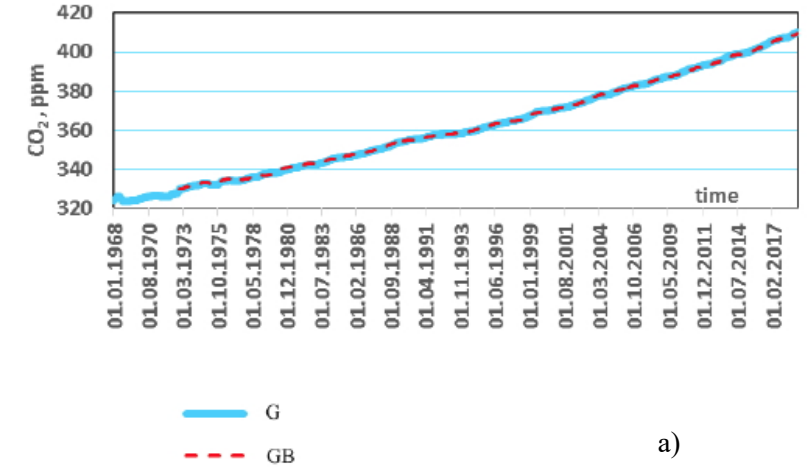

a)

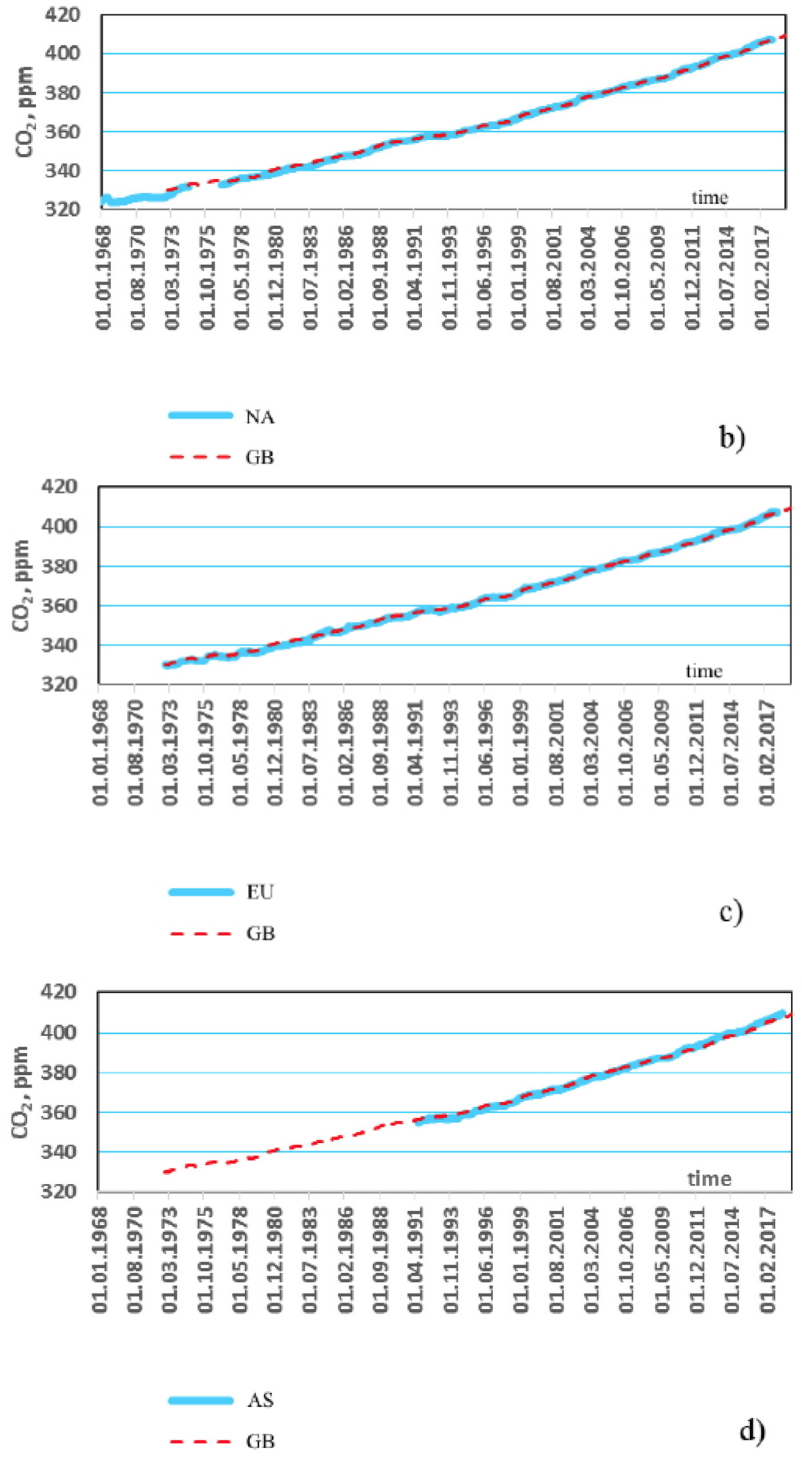

Figure 4. Long-term trends in CO_2 content (ppm) in the near-surface layer of the atmosphere at monitoring stations:
the average for all global stations (GB) and individual variations for all stations (G), North American stations (NA), European stations (EU) and Asian stations (AS)

As seen in Fig. 4, at all stations under consideration long-term trends in CO_2 content (ppm) in the near-surface layer of the atmosphere practically coincide with the global trend (note non-linearity of the trend due to discernible acceleration of concentration rise in the 21st century!).

This coincidence, however, does not mean that absolute levels are identical at all stations. It is hardly expectable given that different areas on the Earth's surface differ not only in the intensity of anthropogenic emissions of CO_2 into the atmosphere, but also in the specific parameters of the processes of absorption and emission of CO_2 by natural oceanic and terrestrial systems, as well as in the intensity of vertical mixing of the atmosphere. Evidence confirms differences in absolute levels. Fig. 5 shows differences $(\overline{B} - \overline{B}_{Alert})$ for all stations under consideration. These values (the calculation method is given above in the Data and Methods section) characterize systematic differences in the level of CO_2 content at all the stations and the Alert station. It is seen in Fig. 5 that at the continental stations in North America and Eurasia, especially in the regions with developed economies, long-term levels of CO_2 content are mainly noticeably higher than the values at the Alert station. At the same time, at the Northern Hemisphere stations located in the lower latitudes and at the island stations, the levels just slightly exceed the levels at the Alert station or are lower than them. In the Southern Hemisphere, long-term CO_2 levels are lower than at the Alert station. As latitude decreases, the differences become more noticeable so that in the extratropical zone they exceed 3 ppm everywhere.

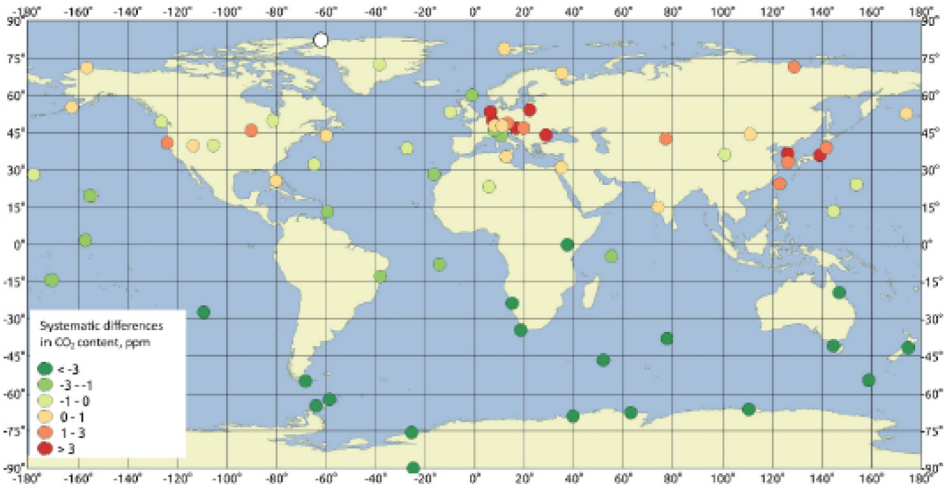

Figure 5. Systematic differences in long-term CO_2 levels (ppm) at different monitoring stations vs. the Alert station

The described picture is quite consistent with the existing concept regarding the following processes involved in the formation of the global CO_2 concentration field: anthropogenic CO_2 emissions associated with economically developed regions (mainly located in the Northern Hemisphere), horizontal atmospheric CO_2 transport (advection), vertical mixing, and partial net-absorption by terrestrial ecosystems and the ocean during advection.

Intra-annual variability

To characterize the intra-annual (inter-monthly) variability of the CO_2 level at a given monitoring station, a series $\{C(n)\}$, $C(n) = A(n) - B(n)$ was employed. The series is obtained through subtracting the long-term trend described by the series of twelve-month running averages $\{B\ (n)\}$ from initial series of monthly mean concentrations $\{A(n)\}$. For an ordered pair of stations, their series $\{C\ (n)\}$ will be characterized by:

– the ratio of the root-mean-square value of *C*-series for the second station to the respective value for the first one;

– the shift of the *C*-series of the second station $\{C\ (n + k)\}$ in time by *k* months[1)], $-5 \le k \le 6$, which ensures the maximum correlation with the series of the first station (the 'optimal shift');

– the value of this maximum correlation.

To exemplify a typical shape of the series $\{C(n)\}$, we displayed the graphs of such series for the stations Alert and Assekrem (a) and for the stations Assekrem and Minamitorishima (b) (Fig. 6). On the panel a), *C*-series for the Assekrem station is shifted by 1 month towards the earlier dates. This is the optimal shift. In Fig. 6, the time on the *X*-axis is measured from the first month for which *C(n)* is available at the Alert station (December 1985). On the panel b), the data for the Assekrem station are represented by dots instead of a line, since otherwise the graphs would be practically indistinguishable.

As Fig. 6 shows, at each station the deviations $C(n)$ are seasonal and similar in different years. The amplitude of oscillations at the Alert station is noticeably larger than at the Assekrem station (panel a)). For the Assekrem and Minamitorishima stations, the amplitudes are almost the same. In both cases, the correlations are 0.94 in spite of the fact that these three stations are not neighbors: Alert is a high-latitude station in the Arctic (82.50°N; 62.34°W; the altitude is 210 m above sea level); Assekrem is a high-altitude station in the north of Africa (23.27°N; 5.63°E; its altitude is 2 710 m above sea level); Minamitorishima (24.29°N; 153.98°E; 7 m above sea level)) is a station on an island in the Pacific Ocean located at the north of the tropical zone. Their elevations are also very different. Nevertheless, the series of deviations $\{C(n)\}$ are quite similar (Fig. 6).

A significant number of stations under consideration do~~es~~ not allow the similar comparison of all stations in pairs within the limited volume of this article. Therefore, only two characteristics will be given below for each station: the root-mean-square value of its series $\{C(n)\}$ and the optimal shift. Both characteristics are relative to the reference Alert station (NOAA) which was chosen arbitrarily.

Fig. 7 shows that the largest root-mean-square values of *C*-series, which presents intra-annual deviations from the long-term trend, are observed in northeastern North America and in Western and Central Europe. In the Arctic, these values are somewhat lower, but still sometimes exceed the value at the Alert

[1)] The shift by *k* months means the transfer from the series $\{C(n)\}$ to the series $\{C\ (n + k)\}$.

station. South of 45°N they become smaller than the values at the Alert station and then noticeably decrease with latitude.

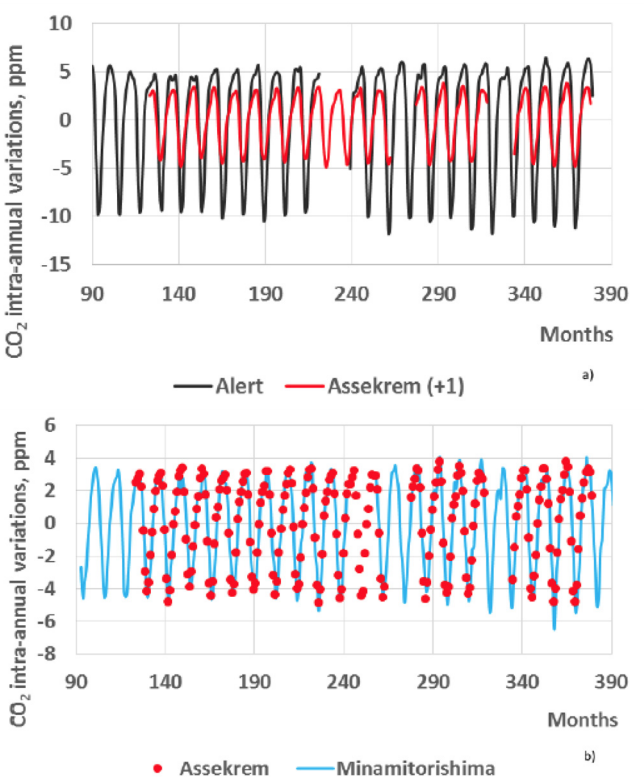

Figure 6. Series {*C*(*n*)} for the stations a) Alert and Assekrem and b) Assekrem and Minamitorishima
On panel a) the series of the Assekrem station is shifted by 1 month towards the earlier dates, which is indicated in the Assekrem legend with (+1)

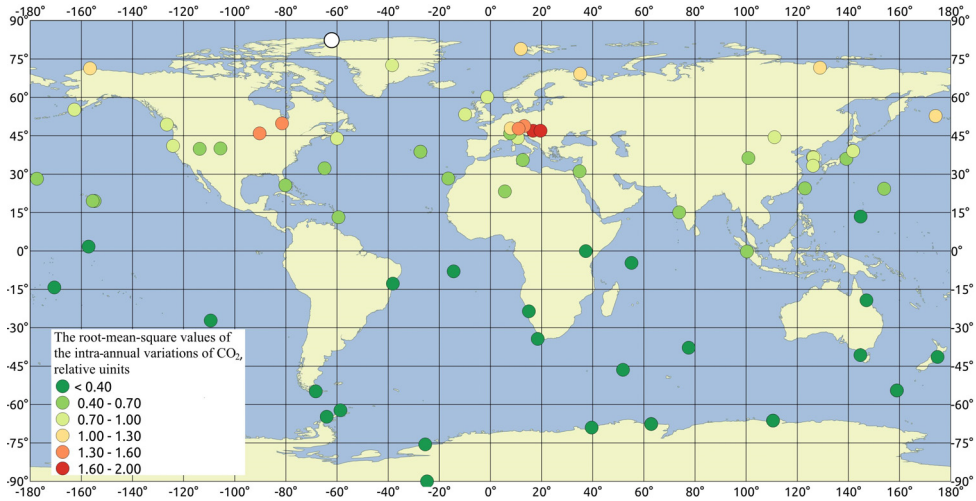

Figure 7. The root-mean-square values of the intra-annual deviations of CO_2 monthly mean concentrations in the atmosphere from the long-term trend at various stations
The root-mean-square value for the Alert station (indicated by the white circle) is taken as a unit

Fig. 8 shows optimal time shifts for different stations in relation to the Alert station, i.e., the time shifts of the $\{C(n)\}$ series for the stations at which the correlation with the series for the Alert station is maximum. In fact, this shift has a seasonal, 'phenological' origin. It apparently reflects the seasonal features of different points of geographical space with respect to the intensity of atmospheric transport processes (both advection and vertical mixing) and the exchange of CO_2 with the underlying surface. At most extratropical stations in the Northern Hemisphere, these intra-annual variations are in phase, i.e., the time shift in relation to the Alert station is 0. At the stations of the tropical zone of the Northern Hemisphere, events are slightly (by 1-2 months) behind of those observed to the north. The series of such stations become similar to the series of the Alert station if respective shifts towards the earlier dates are applied. At most stations located in the Southern Hemisphere, events occur later than at the Alert station, i.e. the series $\{C(n)\}$ of these stations become similar to the series of the Alert station having been shifted towards the earlier dates. The optimal time shift in the Southern Hemisphere is positive and generally increases if the latitude decreases.

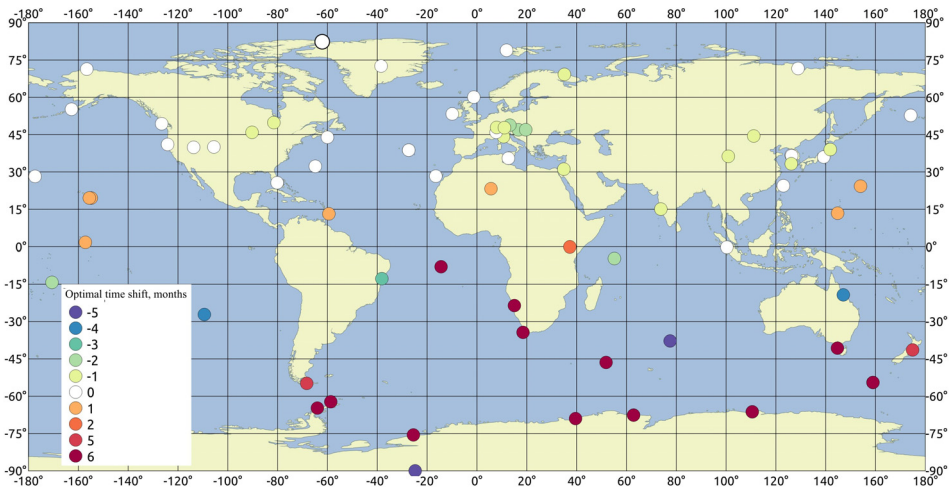

Figure 8. The optimal time shift (months) for the series of intra-annual deviations of CO_2 monthly mean concentrations from the long-term trend for different stations vs. the Alert station series

When searching for the values of the optimal time shift in relation to the Alert station on the segment [-5; 6], they occurred negative for few stations in the South Hemisphere. Perhaps it would be expedient to adjust them by adding 12 months, bearing in mind the 12-month cyclicity of the intra-annual variations. The values of the optimal time shift corrected in this way would be more in harmony with the positive shifts at other stations of the Southern Hemisphere. However, we did not make such color changes for those stations in Fig. 8.

As discussed above in the comments to Fig. 6, after respective time shifts having been applied, the series of intra-annual (inter-monthly) variations can show high correlations even for the stations located at a distance of thousands of kilometers from each other. Let us try to assess all the correlations of the station series $\{C(n)\}$ after applying the optimal time shifts, which, as mentioned above, are

of the seasonal nature. Due to the great number of stations, it is technically impossible to visualize the correlations for all pairs of stations. Therefore, the clustering is performed using the following algorithm.

Let us start from a randomly selected station. Let us continue random sorting through the stations**;** when the absolute value of a station *C-series* optimal time shift in relation to the first station selected is not greater than 1, this station is included into the cluster. Then again, we randomly sort through the remaining stations and stop at the station where the absolute value of the optimal time shifts of its C-series in relation to both already selected stations does not exceed 1. We shall repeat this operation until we cannot find the next station where the optimal time shifts of its *C*-series in relation to all previously selected stations are not greater than 1. The selected stations comprise the 1st cluster. Then we delete its elements from the entire set of stations, and apply the same procedure of clustering to the set of remaining stations starting with a randomly selected station. In this way the 2nd cluster is formed, etc.

As a result, we obtain a partition of the entire initial set of N stations into clusters consisting of n_1, n_2, ..., n_M stations. Within each cluster, the absolute value of the optimal time shift of station series $\{C(n)\}$ for any pair of stations does not exceed 1, i.e. they are 'phenologically similar'.

The result of clustering with the described procedure may change when repeated. Therefore, we repeated it 30,000 times and chose the option of partitioning into clusters, which is characterized by the minimum of the entropy criterion:

$$H = -\sum_{m=1}^{M} \left(\frac{n_m}{N}\right) \ln\left(\frac{n_m}{N}\right).$$

This corresponds to the idea of the greatest ordering of the partition.

In the case under consideration, this clustering procedure revealed 10 clusters, see Fig. 9. The inter-cluster and intra-cluster mean values of correlations found at the optimal time shift were calculated for them. For the intra-cluster correlations, only pairs of different series were taken into account in the calculations. Table 2 shows the intra-cluster and inter-cluster mean values of correlations for clusters 1 to 5. Almost 90% of all stations belong to these clusters. The table 2 shows that both intra-cluster and inter-cluster averages can be rather high, 0.8 and more. This indicates the similarity of intra-annual variations in the levels of CO_2 at the points in space that are remote for considerable distances. Of course, lower values may also occur, since global factors of variability can be masked by local and regional factors specific to the stations.

Table 2. Intra-cluster and inter-cluster average correlations of station series of intra-annual deviations of CO_2 levels from the long-term trend for clusters 1–5; the values are rounded

Clusters	1	2	3	4	5
1	0.90	0.80	0.71	0.85	0.87
2	0.80	0.71	0.68	0.78	0.78
3	0.71	0.68	0.82	0.76	0.74
4	0.85	0.78	0.76	0.95	0.89
5	0.87	0.78	0.74	0.89	0.89

Figure 9. The result of clustering the set of stations. Numbers denote the cluster to which a station belongs

Conclusions

An empirical analysis of the time series of monthly mean CO_2 concentrations for various monitoring stations showed their similarity. Despite differences in the absolute levels of CO_2 content in the near-surface layer of the atmosphere, the long-term trends in the level of CO_2 content are similar even for stations located at a considerable distance from each other. The intra-annual variations have rather high correlative similarity that manifests itself if respective optimal seasonal time shifts are applied. Apparently, in the formation of features of the CO_2 concentration field in the near-surface layer of the atmosphere on the monthly time scale, seasonal local and regional processes of CO_2 exchange with the underlying surface as well as and vertical mixing processes play a greater role than horizontal transfer processes. However, the study of this issue is possible only with a dynamic atmospheric transport model. The empirical analysis is not sufficient.

References

Kyoto Protocol. 1997. Kyoto Protocol to the United Nations Framework Convention on Climate Change. (in Russian) https://www.un.org/en/documents/decl_conv/conventions/kyoto.shtml.

Paris agreement. United Nations. 2015, 32 pp. (in Russian) https://unfccc.int/sites/default/files/russian_paris_agreement.pdf.

UNFCCC. 1992. United Nations Framework Convention on Climate Change, United Nations. 1992. FCCC / INFORMAL / 84 GE.05-62222 190705 280705, 30 pp. (in Russian).

Semenov S.M. 2018a. Sixty years of global monitoring of background atmospheric CO_2 concentrations. − *Fundamental and Applied Climatology*, vol. 1, pp. 5-9, DOI: 10.21513 / 2410-8758-2018-1-05-09 (in Russian).

Semenov S.M. 2018b. Similarity of present-day variations in methane background concentrations in the surface layer of the atmosphere at different latitudes. – *Fundamental and Applied Climatology*, vol. 3, pp. 124-137. DOI:10.21513/2410-8758-2018-3-124-137.

Semenov S.M., Ran'kova E. Ya. 2018. The features of multiyear changes and seasonal variability of present-day background concentrations of CO_2, CH_4, and N_2O at the global monitoring stations. – *Fundamental and Applied Climatology*, vol. 4, pp. 105-121. DOI: 10.21513/2410-8758-2018-4-105-121.

IPCC 2018. Summary for Policymakers. In: Global Warming of 1.5°C. An IPCC Special Report on the impacts of global warming of 1.5°C above pre-industrial levels and related global greenhouse gas emission pathways, in the context of strengthening the global response to the threat of climate change, sustainable development, and efforts to eradicate poverty [Masson-Delmotte, V., P. Zhai, H.-O. Pörtner, D. Roberts, J. Skea, P.R. Shukla, A. Pirani, W. Moufouma-Okia, C. Pjan, R. Pidcock, S. Connors, J.B.R. Matthews, Y. Chen, X. Zhou, M.I. Gomis, E. Lonnoy, T. Maycock, M. Tignor, and T. Waterfield (eds.)]. In press. https://www.ipcc.ch/sr15/.

Keeling C.D., Piper S.C., Bacatow R.B., Wahlen M., Whorf T.P., Heimann P.M., Meijer H.A. 2005. Atmospheric CO_2 and $^{13}CO_2$ exchange with the terrestrial biosphere and oceans from 1978 to 2000: observations and carbon cycle implications. – In: "A History of Atmospheric CO_2 and its effects on Plants, Animals, and Ecosystems" /editors Ehleringer, J.R., T.E. Cerling, M.D. Dearing. – New York, Springer Verlag, pp. 83-113.

Le Quéré C., Andrew R.M, Friedlingstein P., Sitch Hauck J., Pongratz J., Pickers P.A, Korsbakken J.I, Peters G.P, Canadell J.G, Arneth A., Arora V.K, Barbero L., Bastos A., Bopp L., Chevallier F., Chini LP, Ciais P., Doney S.C, Gkritzalis T., Goll D.S, Harris I., Haverd V., Hoffman F.M, Hoppema M., Houghton R.A, Hurtt G., Ilyina T., Jain A.K, Johannessen T., Jones C.D, Kato E., Keeling R.F, Goldewijk K.K, Landschützer P., Lefèvre N., Lienert S., Liu Z., Lombardozzi D., Metzl N., Munro D.R, Nabel JEMS, Nakaoka S., Neill C., Olsen A., Ono T., Patra P., Peregon A., Peters W., Peylin P., Pfeil B., Pierrot D., Poulter B., Rehder G., Resplandy L., Robertson E., Rocher M., Rödenbeck C., Schuster U., Schwinger J., Séférian R., Skjelvan I., Steinhoff T., Sutton A., Tans P.P, Tian H., Tilbrook B., Tubiello F.N, van der Laan-Luijkx I. T., van der Werf G. R., Viovy N., Walker A. P., Wiltshire A. J., Wright R., Zaehle S., Zheng B. 2018. Global Carbon Budget 2018. Earth Syst. Sci. Data 10-2141–2194 https://doi.org/10.5194/essd-10-2141-2018 2018.

The State of Greenhouse Gases in the Atmosphere Based on Global Observations through 2017. 2018, WMO Greenhouse Gas Bulletin. World Meteorological Organization. Global Atmosphere Watch, 8 p. ISSN 2078-0796.

Referencing this paper:

Semenov S.M., Kuzovkin V.V. 2020. Current carbon dioxide content in the near-surface layer of the Earth's atmosphere: long-term trends and intra-annual variability. – *Fundamental and Applied Climatology*, vol. 1, pp. 119-133. DOI: 10.21513/2410-8758-2020-1-119-133

Translation from Russian. The original is published in:
Fundamental and Applied Climatology. 2019, vol. 4, pp. 101-119. DOI:10.21513/0207-2564-2019-4-101-119.